ORIGINAL ARTICLE

Received: August 2018
Accepted: August 2018

Nanohybrid Platform of Functionalized Graphene Oxide for Chemo-Photothermal Therapy

Mohadeseh Hashemi[1,*], Meisam Omidi[2], Javad Mohammadi[1], Mohammad Shalbaf[2], Javad Shabani Shayeh[2], Mohammad Ali Mohagheghi[3]

1. Faculty of New Science and Engineering, The University of Tehran, Tehran 1439957131, Iran.
2. Protein Research Centre, Shahid Beheshti University, GC, Velenjak, Tehran 1985717443, Iran.
3. Tehran University of Medical Sciences, Cancer Research Center, Tehran, 1419733141, Iran.

***Corresponding Author:**
Javad Mohammadi
Faculty of new Science and Engineering, The University of Tehran, Tehran 1439957131, Iran.
Tel:(+98)9128112847
Email: drjmohammadi@yahoo.com

BCCR
2018; 10(4):1-8
www.bccrjournal.com

ABSTRACT

Background: Despite the enormous effort has been done for cancer therapy, fabricating targeted drug delivery platform which can effectively eliminate cancer is a challenge. **Methods**: In this study, we have developed a novel platform composed of graphene oxide (GO), poly-l-lysine (PLL), Herceptin (Her) and doxorubicin (DOX) for chemo-photothermal therapy. GO has been prepared using the hummers method. The morphology of the prepared carriers has studied using transmission electron microscopy (TEM) and scanning electron microscopy (SEM). The successful conjugation of PLL and Her to the surface of GO has been examined using Fourier-transform infrared spectroscopy (FTIR). DOX loading on GO sheets was characterized using UV-Vis absorption spectra. MTT and live/dead assay have been administrated to study the synergistic chemo-photothermal therapy potential of the carries. **Results:** FTIR shows the successful conjugation of the PLL and Herceptin to the GO surface. TGA analysis suggests that, in comparison to GO, GO-PLL has higher thermal stability. In addition, DOX loading efficiency is around 78.5 ± 4.3 %. Also, Live /dead and MTT assays reveal that the introduced carrier can effectively kill cancerous cells via chemo-photothermal effects. **Conclusion**: Our results have suggested that the novel carrier is a versatile platform for chemo-photothermal therapy application.

Keywords: Herceptin, ploy (L-lysine), graphene oxide, graphene oxide

INTRODUCTION:

Graphene oxide (GO) is a two-dimensional hexagonal lattice structure of carbon atoms, which has been employed for various applications such as batteries[1, 2], transistors[1-3] and in biology[4]. Furthermore, GO is considered as an ideal platform for chemo-photothermal therapy due to its high number of functional groups, high aspect ratio, low production cost and satisfactory thermal conductivity[5-8]. However, few studies have focused on the application of GO in chemo-photothermal therapy. Cheng et al. examined the synergistic photothermal effect of PEGylated GO sheets and Doxorubicin (DOX)[5]. Robinson et al. studied the antitumor effect of PEGylated reduced GO on cancer cell lines[6,7]. Hashmi et al. conjugated R9 and Arginine peptide to the surface of reduced GO[8,9]. Even though GO has some promising properties for chemo-photothermal therapy application, the use of GO has been limited due to its low stability in an aqueous media[10-14].

To overcome these obstacles, various biological or synthetic molecules have been used to increase the stability of GO such as TAT[15], pVEC[16], R9[8,17] and poly-l-Arginine[18,19]. Poly-l-lysine (PLL) is an important polymer found in protein foods which can improve the cellular uptake of the carriers it is attached to[20].

In this work, a novel targeted carrier composed of Herceptin (Her) antibody functionalized PLL conjugated GO loaded DOX was synthesized. To meet this goal, we first conjugated PLL to the surface of GO (GO-PLL). Afterwards, Her was conjugated to the surface of GO-PLL (GO-PLL-Her). Finally, DOX was loaded to the GO-PLL-Her to form GO-PLL-Her-DOX.

METHODS:

GO synthesis

GO was synthesized using Hammer's method[21]. 4 grams of graphite powder was oxidized using 12 ml of H_2SO_4 and 2.5 g of P_2O_5 after 4.5 h of stirring at 80°C. Then, graphite oxide was neutralized and immersed in 120 ml of sulfuric acid. Subsequently, 15 g of KM_nO_4 was gradually added to the solution while the temperature was kept under 20°C. Afterwards, the temperature was increased to 40°C while stirring for 2 h, followed by the addition of 700 ml deionized water. The prepared GO was washed to remove excess metal particles. Finally, GO was purified using a dialysis bag (7000 Da) for the duration of one week.

PLL Functionalized GO (GO-PLL)

The GO suspension was sonicated for 2 h (60 W, Misonix, USA). Then, graphene conjugated PLL (GO-PLL) was obtained by stirring 2 mg of GO, 8 mg of PLL, and 10 mg of KOH in 10 ml of distilled water for 24 h at 70°C[22]. Following that, the GO-PLL suspension was washed by centrifugation (5000 rpm for 10 min, Hitachi, Japan).

Herceptin conjugated to GO-PLL (GO-PLL-Her)

1 mL EDC/Sulfo-NHS solution (0.08 M) was added to the GO-PLL (1 mg/ml). After 15 min, Herceptin with a concentration of 0.07 mg/ml was added to the GO-PLL and left for 2 h at room temperature. Unconjugated Herceptin was removed using serial centrifugation.

DOX loading on GO-PLL-Her (GO-PLL-Her-DOX)

DOX was dissolved in DMSO with a concentration of 1.5 mg/ml and then mixed with 0.5 mg/ml of GO-PLL. GO-PLL-Her-DOX was then washed by centrifugation (4000 rpm) to remove unloaded DOX. The loading efficiency of DOX on GO-PLL-Her-DOX was analyzed using UV-vis spectroscopy at 480 nm.

Instrumentation

Surface morphology was examined by transmission electron microscopy (TEM, Zeiss, EM10C) and scan-

ning electron microscopy (SEM, Hitachi S-5500 SEM/STEM, Japan). Fourier transform infrared (FTIR) was recorded using a Spectrum RX I (PerkinElmer). The X-ray diffraction (XRD, PANalytical, Netherlands) was achieved using Cu Kα radiation source. UV-vis spectroscopy was performed (Infinite M200, Tecan Systems Inc., USA). Thermogravimetric analysis (TGA) was carried out using a thermogravimetric analyzer (TGA Q500, Delaware).

GO-PLL-Her-DOX photothermal response

GO-PLL-Her-DOX with a different concentration was transferred to a 96-well plate. The samples were irradiated with an 808nm diode laser with variable power densities (1, 2, 4 and 8 $W.cm^{-2}$). Increasing temperature was monitored using an InSb IR camera. Light emitted from the tip of multimodal optical fiber was imaged to a 6 mm diameter circular spot.

In vitro chemo-photothermal therapy

The Chemo-photothermal therapy potential of GO-PLL-Her-DOX was evaluated on the BT474 cell line using MTT and live/dead assays. Cells (50,000 cells/well) were seeded in a 96-well plate overnight. Then, the medium was replaced with complete DMEM containing various DOX concentrations (0,1.25, 2.5, 5, 10, 20 $\mu g.ml^{-1}$) in the form of free DOX and GO-PLL-Her-DOX for 24 h. After that, the laser groups cells were exposed to NIR light laser (8 W/cm^2, 5 min). Cell viability was measured using MTT assay[23].

Live/dead assay was used to visualize the effect of GO-PLL-Her-DOX on BT474 cell lines. 50,000 cells/well were seeded in a 96-well plate. After 24 h, cells were treated using 15 mg/ml of GO-PLL-Her-DOX. After another 24 h, cells were washed with PBS (3 times) followed by exposure to NIR irradiation (8 W/cm^2, 5 min). After one hour of incubation, cells were stained using calcein AM (2 M) and ethidium homodimer-1 (EthD–1) (4 M) for 15 min. Images were taken using an inverted fluorescent microscope (Evos, Life Technologies).

RESULTS & DISCUSSION:

The morphology of synthetic GO was examined using TEM and SEM. As shown in **Figure 1A** and **B**, the morphology of GO was smooth and regular. Successful conjugation of PLL to the GO surface was examined using FTIR. As shown in **Figure 1C**, the GO spectrum showed characteristic peak at 3440 cm^{-1}, 1733 cm^{-1}, 1614 cm^{-1} and 1085 cm^{-1} which corresponded to the stretching vibration of O–H, C=O, C=C and C–O bonds, respectively. The FTIR spectrum of GO-PLL exhibited GO-PLL absorption feathers, for example C–N at 1313 cm^{-1}, C=O at 1624 cm^{-1} and N-H at 3278 cm^{-1}.

After confirming GO-PLL formation, FTIR spectrum was used to confirm the conjugation of Her to the GO-PLL surface (GO-PLL-Her). As shown in **Figure 2A**, the GO-PLL-Her spectrum represented the formation of a new peak at around 1540 cm^{-1} which is related to the amide groups and confirmed GO-PLL-Her development. Also, decreasing the intensity of carboxyl groups (~3443 cm^{-1}) leads to the reduction of GO-PLL during conjugation of Her.

The UV-vis absorption spectrum of DOX, GO-PLL and GO-PLL-Her-DOX were shown in **Figure 2B**. DOX is an aromatic and hydrophobic drug which could be loaded onto the surface of GO via hydrophobic-hydrophobic and π-π stacking interactions[24]. As shown in **Figure 2B**, the presence of DOX absorption feathers on the surface of GO-PLL-Her confirmed GO-PLL-Her-DOX formation. UV-Vis absorption analysis also showed that the amount of DOX loaded onto the surface of GO-PLL-Her-DOX was around 78.5 ± 4.3 %. The stability of GO-PLL-Her-DOX was studied using TGA thermogram. As shown in **Figure 2C**, two-large shoulders in the TGA thermogram were located at around 150 and 300°C. Weight loss at a temperature less

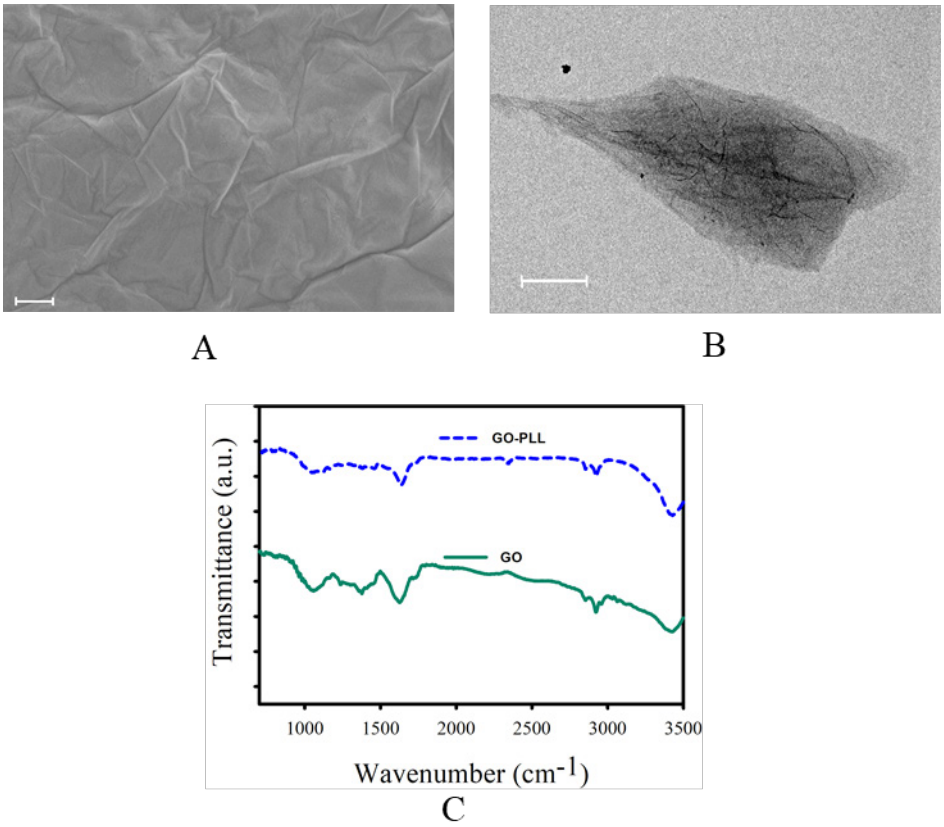

Figure **1. A**. SEM and **B**. TEM images of GO (The scale bar is 500 nm), C) FTIR spectrum of GO and GO-PLL,

than 100°C was related to moisture evaporation while weight loss between 150-270°C led to PLL melting[25]. In the GO-PLL thermogram, the amount of weight loss at a temperature less than 100°C is 4% more than GO, which may lead to incomplete drying due to the presence of heavy chain PLL. At a range of 100-200°C, GO and GO-PLL showed 34% and 26% weight loss, respectively. This may be attributed to the presence of labile oxygen in the structure which decreased due to the conjugation of PLL to the GO surface[25-27]. Weight loss between 300 to 400°C could be related to PLL evaporation[25]. Furthermore, weight loss above 350°C could be related to carbon pyrolization[25-27]. As shown in **Figure 2C**, the slope of the GO-PLL thermogram was lower than GO, indicating that the decomposition rate of GO-PLL is lower than GO at a temperature between 50 to 200°C.

The morphology of the synthesized GO-PLL-Her-DOX was studied using SEM. As shown in Figure 2D, the morphology of GO-PLL-Her-DOX had clearly changed after conjugation and there were no visible individual sheets. Similar morphology was observed by

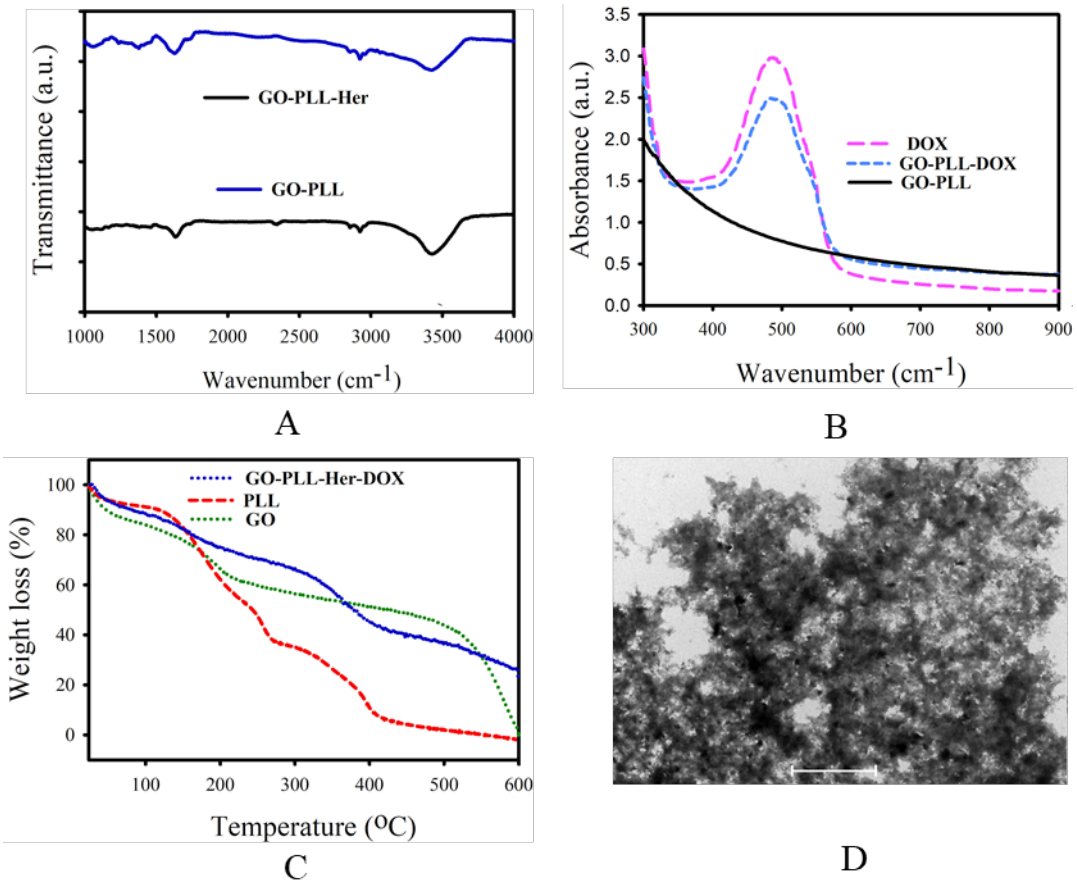

Figure **2. A**. FTIR spectrum of GO and GO-PLL, **B**. UV-Vis absorption spectra of DOX, GO-PLL, GO-PLL-Her-DOX, C) TGA spectra of GO, GO-PLL, GO-PLL-Her, DOX, D) SEM image of GO-PLL-Her-DOX

Ewa et al[28] and Hashemi et al[22,29].

After physio-chemical characterization of GO-PLL-Her-DOX, the photothermal behavior of the carriers was studied during NIR laser irradiation. As shown in **Figure 3A**, the temperature increase was dependent on the carrier's concentration. As the concentration increased, there was an increase in the amount of temperature raised. However, the temperature increase for water as a control sample was 0.16 ± 0.1°C. The photothermal behavior of the carriers was power density dependent. As shown in **Figure 2C**, the temperature increase for 15 mg/ml of GO-PLL-Her-DOX with a power density of 8 w/cm^2 was 30.2 ± 2.1°C which was sufficient for photothermal therapy. Afterwards, the chemo-photothermal behavior of GO-PLL-Her-DOX was studied using MTT and live dead assay on the BT-474 cell line. As shown in **Figure 3B**, BT-474 cells were treated with various DOX concentrations in the form of free DOX and GO-PLL-Her-DOX with and without NIR laser irradiation (5 min, 8 W.cm^{-2}). All groups showed concentration-dependent toxicity. Furthermore, to visualize the chemo-photothermal effect

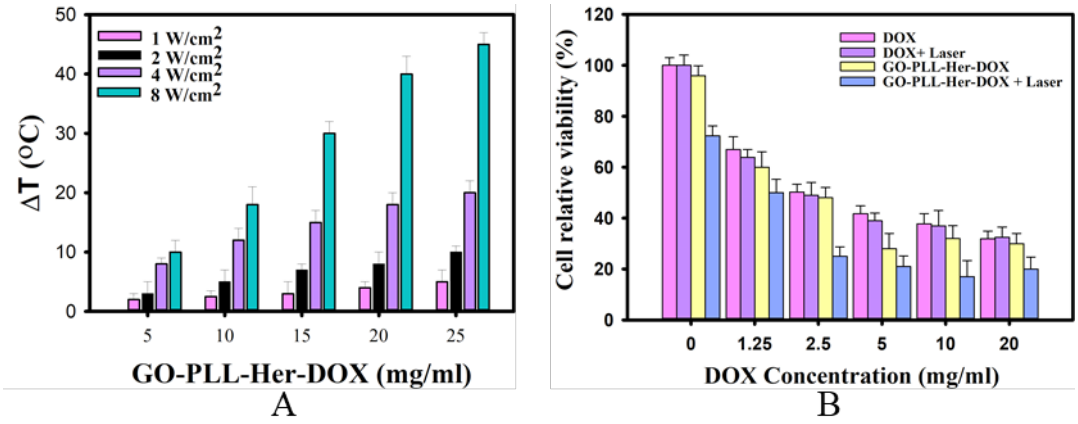

Figure **3. A**. The photothermal response of various concentrations of GO-PLL-Her-DOX at different power densities (1, 2, 4, 8 W/cm^2), **B**. In vitro cell toxicity of various DOX concentration in the form of free DOX and GO-PLL-Her-DOX

of GO-PLL-Her-DOX, a live/dead assay was applied to the BT-474 cell lines. As shown in F**igure 4**, dead cells exhibited red fluorescent light while live cells radiated green fluorescence. In the group treated with GO-PLL-Her-DOX nanoparticles, there was an increase in dead cells compared to the control group, representing the antitumor effect of GO-PLL-Her-DOX[30].

CONCLUSION:

GO-PLL-Her-DOX, a dual chemo-photothermal therapy carrier was successfully prepared. GO served two purposes, first as a photo-transducer which absorbed NIR light and converted it to heat, and second as a carrier for loading DOX. The morphology of the carrier was examined using SEM and TEM, and the successful conjugation of PLL and Her to the GO surface was studied using FTIR. Furthermore, the thermal stability of the samples was analyzed using TGA. Finally, MTT and live/dead assay were administrated to study the chemo-photothermal effect of GO-PLL-Her-DOX on BT-474 cells. Our results suggest GO-PLL-Her-DOX as a potential candidate for chemo-photothermal therapy.

REFERENCES:

1. Novoselov KS, Geim AK, Morozov SV, Jiang D, Katsnelson MI, Grigorieva IV, et al. Two-dimensional gas of massless Dirac fermions in graphene. Nature. 2005;438(7065):197-200.
2. Schwierz F. Graphene transistors. Nat Nanotechnol. 2010;5(7):487-96.
3. Sun J, Lee HW, Pasta M, Yuan H, Zheng G, Sun Y, et al. A phosphorene-graphene hybrid material as a high-capacity anode for sodium-ion batteries. Nat Nanotechnol. 2015;10(11):980-5.

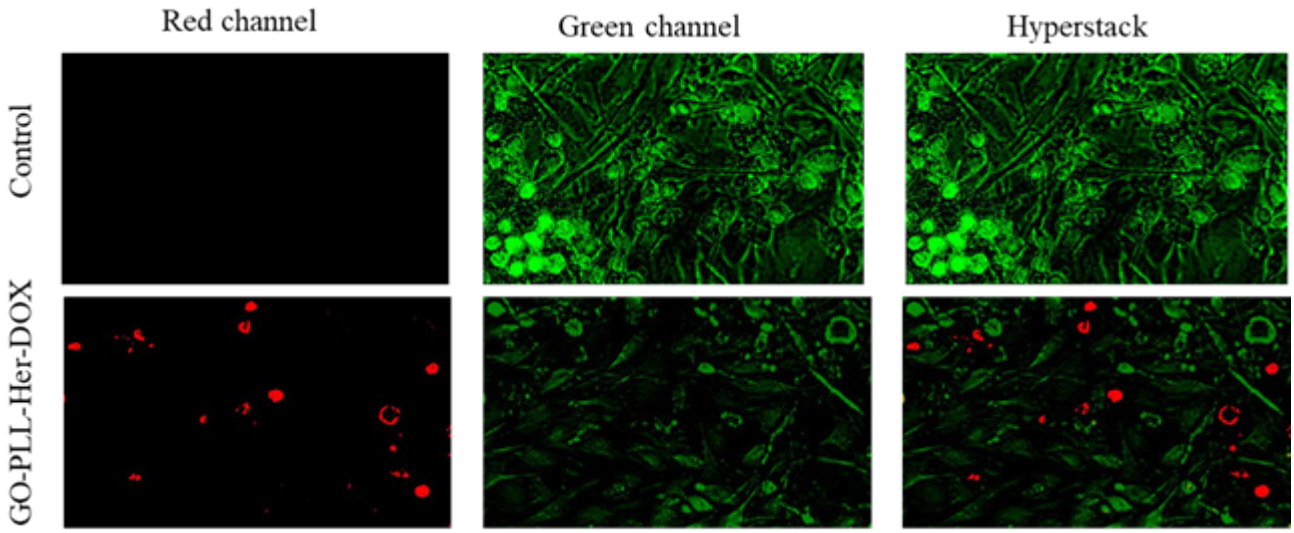

Figure 4. Study the chemo-photothermal effect of GO-PLL-Her-DOX on BT-474 cell lines.

4. Chung C, Kim YK, Shin D, Ryoo SR, Hong BH, Min DH. Biomedical applications of graphene and graphene oxide. Acc Chem Res. 2013;46(10):2211-24.
5. Zhang W, Guo Z, Huang D, Liu Z, Guo X, Zhong H. Synergistic effect of chemo-photothermal therapy using PEGylated graphene oxide. Biomaterials. 2011;32(33):8555-61.
6. Robinson JT, Tabakman SM, Liang Y, Wang H, Casalongue HS, Vinh D, et al. Ultrasmall reduced graphene oxide with high near-infrared absorbance for photothermal therapy. J Am Chem Soc. 2011;133(17):6825-31.
7. Li D, Kaner RB. Materials science. Graphene-based materials. Science. 2008;320(5880):1170-1.
8. Hashemi M, Yadegari A, Yazdanpanah G, Jabbehdari S, Omidi M, Tayebi L. Functionalized R9–reduced graphene oxide as an efficient nano-carrier for hydrophobic drug delivery. RSC Advances. 2016;6(78):74072-84.
9. Hashemi M, Omidi M, Muralidharan B, Smyth H, Mohagheghi MA, Mohammadi J, et al. Evaluation of the Photothermal Properties of a Reduced Graphene Oxide/Arginine Nanostructure for Near-Infrared Absorption. ACS Appl Mater Interfaces. 2017;9(38):32607-20.
10. Hu H, Wang X, Lee KI, Ma K, Hu H, Xin JH. Graphene oxide-enhanced sol-gel transition sensitivity and drug release performance of an amphiphilic copolymer-based nanocomposite. Sci Rep. 2016;6:31815.
11. Singh SK, Singh MK, Nayak MK, Kumari S, Shrivastava S, Gracio JJ, et al. Thrombus inducing property of atomically thin graphene oxide sheets. ACS Nano. 2011;5(6):4987-96.
12. Singh SK, Singh MK, Kulkarni PP, Sonkar VK, Gracio JJ, Dash D. Amine-modified graphene: thrombo-protective safer alternative to graphene oxide for biomedical applications. ACS Nano. 2012;6(3):2731-40.
13. Shim G, Kim JY, Han J, Chung SW, Lee S, Byun Y, et al. Reduced graphene oxide nanosheets coated with an anti-angiogenic anticancer low-molecular-weight heparin derivative for delivery of anticancer drugs. J Control Release. 2014;189:80-9.
14. Stankovich S, Dikin DA, Piner RD, Kohlhaas KA, Kleinhammes A, Jia Y, et al. Synthesis of graphene-based nanosheets via chemical reduction of exfoliated graphite oxide. carbon. 2007;45(7):1558-65.
15. Vives E, Brodin P, Lebleu B. A truncated HIV-1 Tat protein

basic domain rapidly translocates through the plasma membrane and accumulates in the cell nucleus. Journal of Biological Chemistry. 1997;272(25):16010-7.

16. Elmquist A, Lindgren M, Bartfai T, Langel U. VE-cadherin-derived cell-penetrating peptide, pVEC, with carrier functions. Exp Cell Res. 2001;269(2):237-44.
17. Futaki S, Suzuki T, Ohashi W, Yagami T, Tanaka S, Ueda K, et al. Arginine-rich peptides. An abundant source of membrane-permeable peptides having potential as carriers for intracellular protein delivery. J Biol Chem. 2001;276(8):5836-40.
18. Madani F, Lindberg S, Langel U, Futaki S, Graslund A. Mechanisms of cellular uptake of cell-penetrating peptides. J Biophys. 2011;2011:414729.
19. Wender PA, Mitchell DJ, Pattabiraman K, Pelkey ET, Steinman L, Rothbard JB. The design, synthesis, and evaluation of molecules that enable or enhance cellular uptake: peptoid molecular transporters. Proc Natl Acad Sci U S A. 2000;97(24):13003-8.
20. Hinshaw J, Prestwich G. The design, synthesis, and evaluation of molecules that enable or enhance cellular uptake: Peptoid molecular transporters. Chemtracts. 2001;14(7):391-4.
21. Xu Y, Bai H, Lu G, Li C, Shi G. Flexible graphene films via the filtration of water-soluble noncovalent functionalized graphene sheets. J Am Chem Soc. 2008;130(18):5856-7.
22. Hashemi M, Omidi M, Muralidharan B, Smyth H, Mohagheghi MA, Mohammadi J, et al. Evaluation of the Photothermal Properties of a Reduced Graphene Oxide/Arginine Nanostructure for Near-Infrared Absorption. ACS Appl Mater Interfaces. 2017;9(38):32607-20.
23. Xiong L, Shen B, Behera D, Gambhir SS, Chin FT, Rao J. Synthesis of ligand-functionalized water-soluble [18F]YF3 nanoparticles for PET imaging. Nanoscale. 2013;5(8):3253-6.
24. Xu Z, Wang S, Li Y, Wang M, Shi P, Huang X. Covalent functionalization of graphene oxide with biocompatible poly(ethylene glycol) for delivery of paclitaxel. ACS Appl Mater Interfaces. 2014;6(19):17268-76.
25. Krikorian V, Kurian M, Galvin ME, Nowak AP, Deming TJ, Pochan DJ. Polypeptide-based nanocomposite: Structure and properties of poly (L-lysine)/Na+-montmorillonite. Journal of Polymer Science Part B: Polymer Physics. 2002;40(22):2579-86.
26. Park S, An J, Potts JR, Velamakanni A, Murali S, Ruoff RS. Hydrazine-reduction of graphite-and graphene oxide. Carbon. 2011;49(9):3019-23.
27. Wang Y, Liu J, Liu L, Sun DD. High-quality reduced graphene oxide-nanocrystalline platinum hybrid materials prepared by simultaneous co-reduction of graphene oxide and chloroplatinic acid. Nanoscale research letters. 2011;6(1):241.
28. Sawosz E, Jaworski S, Kutwin M, Vadalasetty KP, Grodzik M, Wierzbicki M, et al. Graphene Functionalized with Arginine Decreases the Development of Glioblastoma Multiforme Tumor in a Gene-Dependent Manner. Int J Mol Sci. 2015;16(10):25214-33.
29. Hashemi M, Omidi M, Muralidharan B, Tayebi L, Herpin MJ, Mohagheghi MA, et al. Layer-by-layer assembly of graphene oxide on thermosensitive liposomes for photo-chemotherapy. Acta Biomater. 2018;65:376-92.
30. Tong L, Wei Q, Wei A, Cheng JX. Gold nanorods as contrast agents for biological imaging: optical properties, surface conjugation and photothermal effects. Photochemistry and photobiology. 2009;85(1):21-32.